

Thermographics measurements and numerical simulation of a car brakes

by M. Kastek*, T. Piatkowski*, H. Polakowski* and J. Małachowski**, J. Jachimowicz**

* Inst. of Optoelectronics, Military Univ. of Technology, gen. S.Kaliski 2 Warsaw Poland, mkastek@wat.edu.pl

**Depart. of Mech. and Applied Comp. Sc., Military University of Technology, gen. S.Kaliski 2 Warsaw Poland

Abstract

This paper presents the test campaign concept and definition and the analysis of the recorded measurements. The braking temperature on a lining surface can rise above 500°C. Experimental tests were conducted on the test machine called IL-68, modified to enable thermographic measurements. The paper presents the results of analysis of thermal images registered at different conditions during the tests as well as results of dynamic tests and calculated thermal parameters characterizing the brake. Furthermore, based on this testing machine, and tests results the numerical model was developed. Computations were performed using a dynamic LS-Dyna code where heat generation was estimated assuming full (100%) conversion of mechanical work done by friction forces.

1. Introduction

Typically, braking from nominal speed to full stop, takes about 5-15s. At that time, most of the kinetic energy of a vehicle is changed into heat generated in brake system [1]. Heat emitted at the working surfaces of brake is causing heat stroke directed into the components of friction pairs. Those rapid temperature changes on the surfaces of brake pads and discs may lead to tribological deformations [3, 4] or even breaking of mating surfaces [1, 2]. This leads usually to premature wearing of brake elements. Moreover the temperature growth diminishes the braking effectiveness and may as well induce unwanted vibrations, known as "hot judder" [6].

The aforementioned effects were discussed in [2, 6, 7]. The application of fast thermal camera for the recording of temperature changes during braking makes it possible to register the changes of temperature distribution on the friction elements. There is, however the problem to provide clear, unobstructed line of sight to the tested elements of the brake. Currently available thermal cameras provide fast image acquisition rates, up to thousands fps in windowed mode. At frame rates greatly surpassing the dynamics of the process the averaging of readings is not an issue any more. Otherwise, for too slow data acquisition rate (in comparison with the speed of recorded process) the averaging leads to the underestimation of both surface temperatures and thermal gradients [8]. The experimental results of brake temperature measurements were presented in [8, 9].

The non-contact measurement of temperature distribution on frictional surfaces is a complicated task, mainly because the emissivity exhibits strong dependence with temperature, which in turn changes in a very broad range through the braking process. Furthermore this dependence is usually unknown [10] and has to be estimated [11, 12]. Such estimation in case of analyzed problem is possible with the error margin not exceeding 3% [13, 14].

Thermal phenomena in the pair brake pad - disc, is particularly important in special vehicles, both civilian and military. Their large masses or high velocities require higher braking forces. Due to permanent deformation in the contact area, increasing load on the direction normal to the contact surfaces causes increase of actual contact surface, up to the maximum value for a given friction pair [15]. This leads to generation of large amount of heat. Operation in extreme conditions, such in mountains, with frequent brakes, can lead to overheating and – in extreme cases – to the destruction of a brake system [16, 17].

The key issue for an engineer designing a new brake is to measure or to predict both average and local temperatures which are key factor in estimation of brake lifetime and effectiveness. In present paper, temperature obtained from experimental and numerical tests are studied. Thermal measurements are used to validate the numerical model of the brake and test stand. The further processing of thermal image data may lead to the improved mechanical construction of the brake.

2. Measurement stand

Experimental tests were conducted in the Institute of Aviation in Warsaw on the test machine called IL-68 and its main elements are shown on the picture below. The main component of IL-68 is so called frictional unit, which consists of: rotational head, which convey a shaft torque and where counter samples are placed, translational head, where samples of coatings are placed and pressed against counter samples, is shown on Fig. 1.

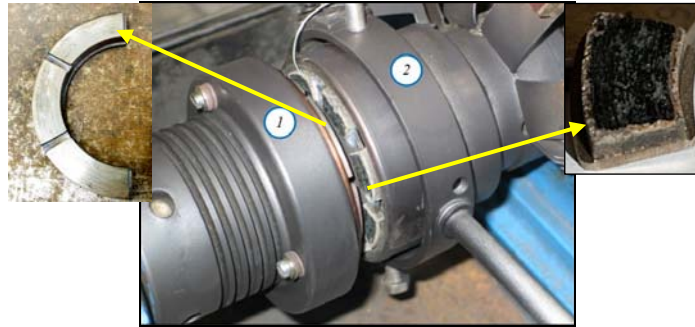


Fig 1: Frictional unit of the IL-68 rig 1. Rotational head, 2. Translational head

The stand allows for examination of frictional pairs without the need of building a full-scale prototype of a brake. Choosing the geometry of tested samples adequately, it is possible to simulate the brake performance, using relatively small objects. Variable rotational speed of shaft, in the range $0 \div 9000$ rpm, allows users to simulate wide range of linear speed in the friction pair. In the described test, it was set at 6000 rpm. Moment of inertia of the rotating masses which simulate the energy dissipation similar to the energy dissipated in the real brake, can be set within the limits of $0.154 \div 1.54 \text{ kg}\cdot\text{m}^2$ and $0.098 \text{ kg}\cdot\text{m}^2$ ($0.412 \text{ kg}\cdot\text{m}^2$ during tests). In addition, force acting on a friction pair can be adjusted from 0 to 5.88 kN. The stand allows to measure the inertia and the clamping force. These measurements are complemented by measurements of temperature distributions using infrared cameras [18].

IL-68 test rig was modified by installing the thermal imaging system. Remote temperature measurements by a thermal camera require a clear view of a measured surface. It was achieved by removing one of tested brake pads and making an opening there which serves as a measurement window. The modification of the test stand is shown in Fig. 2.

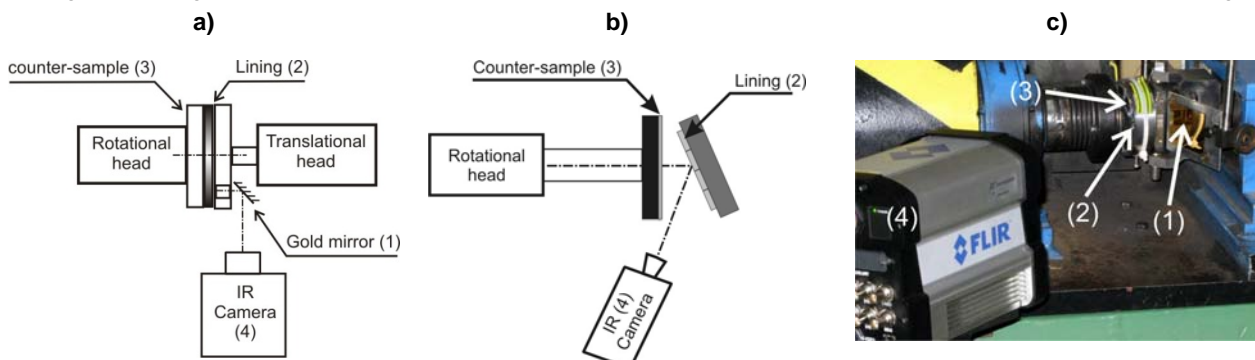


Fig. 2. Additional thermal imaging system: block diagram during test (a), block diagram during cooling (b), real photo of a modified test rig (brake elements disconnected) (c).

Additional mirror (1) was applied due to the lack of free space to mount the thermal camera directly in front of a measurement window and to prevent the possible lens damage by brake pads debris. Due to the high rotational speeds and thus the rapid changes in temperature field, the infrared camera ThermoCAM SC6000 was used for testing [13, 19]. Data were recorded in a reduced frame, matched to the dimensions of measurement window. Camera allows to write data at speeds up to 1000 reduced frames per second. Reduction of amount of data - i.e. area of measurement, was forced by the maximum data transfer rate in "Fast Speed" mode that can be reached for the applied camera. Due to the high dynamics of the signal, measurements were carried out in the measuring range $200^{\circ}\text{C} \div 600^{\circ}\text{C}$ [18, 20]. Thus, in the initial phase of test, in the absence of friction, and at the very end of the brake cooling, data from infrared camera were not available. Spatial resolution for given focal length, distance from camera to sample and detector pixel pitch is $0.1 \times 0.12 \text{ mm}$.

3. Thermographic measurements

Thermal measurements were performed in different configurations. In the first one (Fig.2a) the temperature profile on the brake disc was measured. It is possible through direct observation of the test sample from relatively short distance. As a result the camera FOV matches the size of the available sample area and the spatial resolution of a camera is optimally utilized. Short viewing distance also makes it possible to neglect the effect of atmospheric attenuation of IR signal on the results of temperature measurements. It should be noted that the resulting image is flipped upside down because of mirror in the optical path. The sequence of thermal images of a brake disc recorded during braking is shown in Fig. 3.

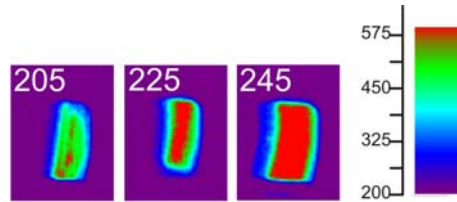


Fig. 3. Thermal images of a brake disc during braking.

From the selected frames 205, 225 and 245 it can be seen how the surface temperature distribution changes during braking. Initially there are several small hot areas, caused by actual shape of the disc and pad surfaces, which are not perfectly flat and local points of contact (and thus heat generation) are present. As the braking continues, the hot area extends over nearly entire surface which indicates full braking power.

The second measurement configuration was used to record the temperature of the temperature of braking pads, when the test machine head was opened (Fig. 2b). This measurement was performed after the full braking cycle had been completed. The settings used for the braking process and environmental data during the measurement session are shown in Table 1.

Table 1. Measurement parameters during the tests

Parameter	Value	Unit
Pressing force	7258	N
Angular velocity	6000	rpm
Average pressure	511	N/cm ²
Braking torque Max	125	Nm
Ambient temperature	18	°C
Humidity	67	%

3.1. Temperature rise during braking cycle

In the first measurement the temperature rise of the braking disc was recorded. In order to precisely determine the temperature rise rate the full acquisition speed of a camera was utilized. The used measurement range of a camera was 200°C to 600°C. Prior to the measurement session the camera was calibrated in the accredited laboratory in the Institute of Optoelectronics, Military University of Technology.

For comparison, the alternative, contact temperature measurements was performed using K-type thermocouples, located 1 mm beneath the outer surface of the brake pads. The recorded plots showing temperature rise versus time are shown in Fig.3, as well as the placement of thermocouples (temperatures T1 and T2). The starting velocity 6000 rpm and the braking lasted till the full stop. The image acquisition rate of a camera was set at 200 Hz. In this case the measurement head was not open after the braking.

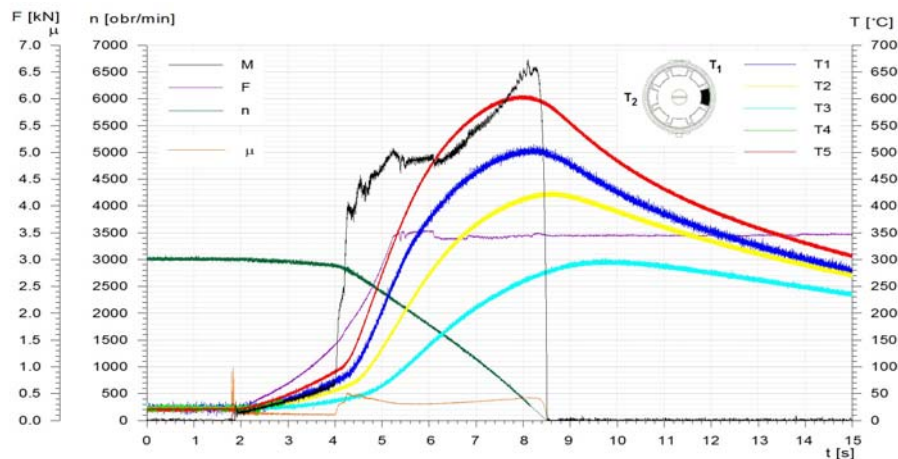


Fig. 3. Changes of temperature T1 - T5, braking momentum M, force F, rotational speed n and friction coefficient μ during braking.

The thermal image data revealed the presence of „hot spots” with temperatures above 600°C. The exact temperature values could not be determined with the actual measurement camera, because higher range is required. The measurement stand is now modified and two camera setup will be used. LWIR camera SC7900 is capable of

calibrated measurements of higher temperatures but with lower resolution. This lowered resolution, however, is not so important in case of hot spot temperatures above 600°C.

The emissivity value can be estimated by comparing the temperatures registered by contact and non-contact methods. The difference in temperature readings is caused by the placement of thermocouple, about 2 mm from the surface viewed by a thermal camera. The sensor cannot be located closer, because it could be damaged, as the braking pads wears out during the braking. Time shift between T and T2 graphs is caused by large time constant of a thermocouple.

3.2. Temperature measurements after the opening of measurement head

The second series of measurements was performed in order to register the brake disc cooling, in a measurement setup shown in Fig. 2b. The cooling rate is considerably slower, so the image acquisition rate was set at 1 frame per second. At this rate the 3 minute long recording could be stored in an internal camera buffer.

The fragment of a tested brake disc is shown in Fig. 4a, whereas Fig. 4b shows the thermal image recorded after stopping and opening the measurement head, when the elements of a friction pair were separated.



Fig. 4. Brake disc (a) and its thermal image on a test stand (b)

The rectangular areas on the thermal image of a brake disc (Fig.4b) are the notches separating the disc areas, which can be seen in Fig. 4a. Their elevated temperatures are in fact caused by higher emissivity of a cavity, so the recorded temperature appears as higher than the neighbor flat surfaces. After correcting this cavity effect the resulting temperature distribution is uniform across the entire brake disc.

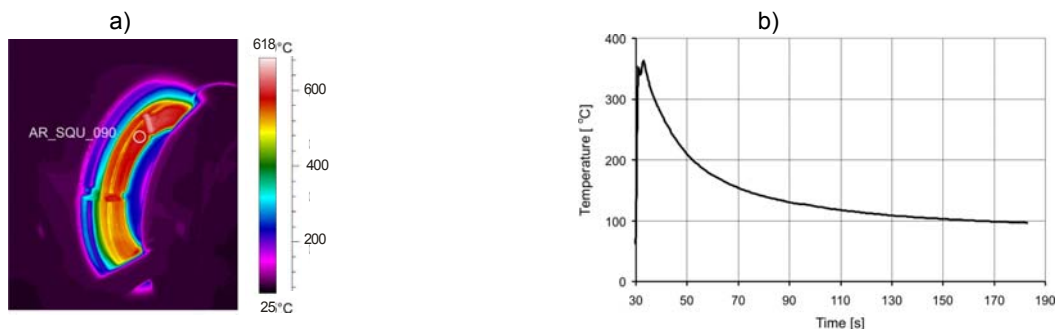


Fig. 5. Cooling of brake disc after the opening of measurement head: (a) thermal image at the beginning of the process, (b) temperature change versus time

The graph showing the cooling of the brake disc is presented in Fig. 5. In this plot the mean temperature of the central area of the tested brake disc is shown (the circular area in Fig.5a). The disc cooling process is recorded after the opening of the measurement head and the resulting graph shows exponential descent. From that part the time constant of the process was determined, a parameter that is further required for numerical modeling of the brake elements.

Cooling characteristics can be approximated using time constant value $\tau_1 = 11,8 \pm 0,8$ s for the initial stage and $52,18 \pm 0,1$ s for the final stage of the cooling process.

The cooling process in the open configuration has smaller time constant than in the real brake because in the experiment heat is transferred by both conduction and radiation. In the real brake the radiation component is smaller. In the late stage of the cooling process the temperature drops at a very low rate and after 6 minutes it still exceeds 150°C. It is an important information for the design of brakes for the vehicles used in difficult conditions (e.g. in the mountain regions). With frequent braking cycles the brake elements cannot be sufficiently cooled, what leads to faster wearing of friction elements. The highest temperature recorded by a thermal camera at different loads was over 600°C.

3.3. Measurements of the temperature of brake pads

The pads were viewed by a thermal camera after the full opening of the measurement head. In this case the observation (and temperature measurement) was performed in the direction normal to the measured surfaces to avoid additional errors. The pads were numbered from 1 to 8, as shown in Fig.6a. The pad 1 has the highest local temperature values.

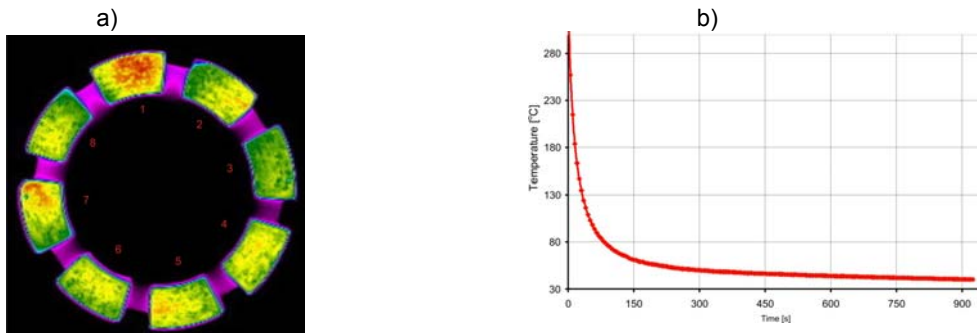


Fig. 6. Temperature distribution on surface of pads (a), temperature change versus time pad 1 (b).

It can be seen from the recorded thermal images that pads (contrary to the disc) are not uniformly heated. The cooling of the pad No1 is shown in fig 7a. This pad has the highest local temperature value as well as highest mean temperature across the entire surface. High temperatures of the tested pad makes it possible to analyze the temperature distribution with high resolution for several profiles. In this case three profiles were analyzed to assess the non-uniformity of temperature distribution on pad 1, as shown in Fig.7b.

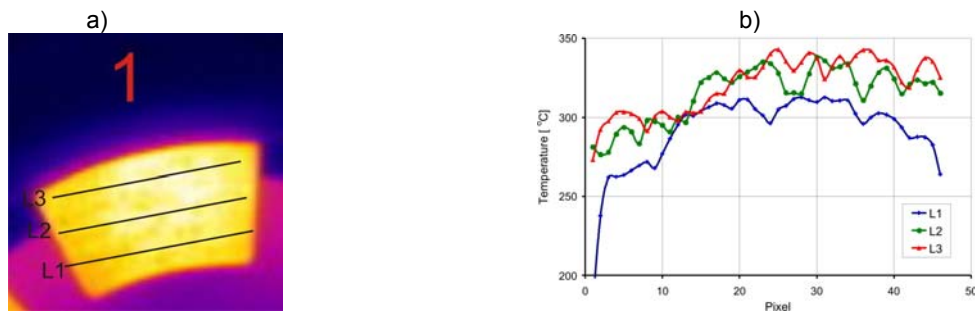


Fig.7. Temperature measurements across the surface of pad 1: selected profiles (a) and measured temperature values (b).

The temperatures along the selected lines L1-L3 are shown in Fig.8a. In spite of differences in absolute temperature values the shape of temperature distribution is similar in all three cases. In order to obtain more accurate description of temperature distribution three additional temperature profiles were measured, this time in the radial direction. The profile lines and corresponding temperature distributions are shown in Fig.8b.

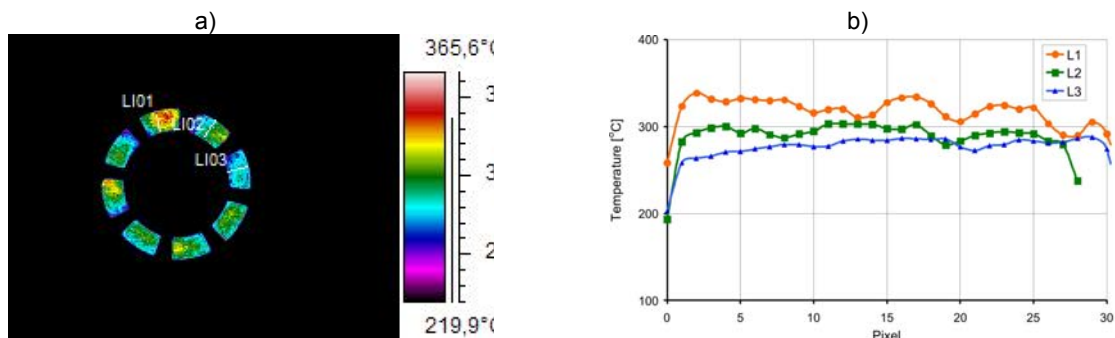


Fig. 8. Radial temperature profiles: location (a), temperature values (b).

It can be seen that the non-uniformity increases with the rise of mean temperature value. Those differences result probably from the local structure of a pad material. The contact surfaces of friction elements are subjected to thermal and mechanical stress and as a result the structure is altered, mainly due to such effects as ridging, abrasion and plastic deformations. The measurement results were then used as input for the numerical modeling of the measurement stand. The maximal values of local temperature differences were determined on the friction surfaces, which reached as high as 80°C. The results of numerical simulations and the comparison between calculated and measured temperature data are presented hereunder.

4. Numerical model of IL-68 stand

As it was already mentioned the temperature measurements by thermal imaging has lead to the development of 3D numerical model of a test stand, making it possible to simulate the temperatures of a friction surfaces during braking at different loads. Finite elements numerical model of the system was developed, with a focus put on frictional unit. More comprehensive description of the model can be found in [21]. Each of the 15 elements of the IL-68 was meshed using hexagonal elements (Fig. 9, Fig. 10).

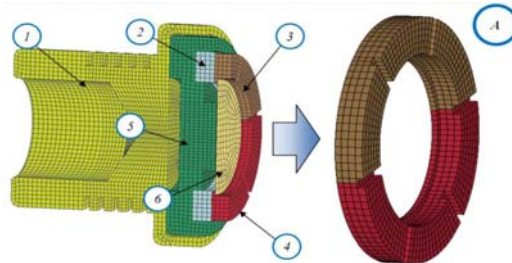


Fig. 9. Numerical model of rotary head detailing the counter-samples: bushing counter-samples, 2) base of the counter-samples, 3 and 4) counter-sample, 5) counter-samples housing, 6) washer

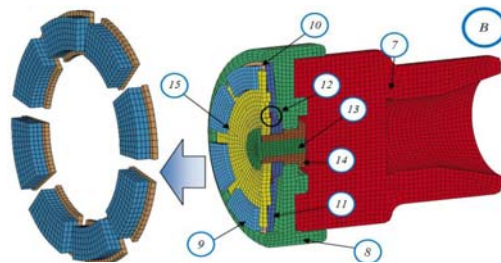


Fig. 10. Numerical model of the translational head, detailing lining samples: 8) samples housing, 9) lining sample, 10) base of the sample, 11) rosette, 12) washer, 13.14), screws, 15) closing cap

Initial and boundary conditions has been defined in a manner that allowed to kinematically force rotation of all components of the braked part (rotational head) and to prevent their sliding along the rotation axis (W1). Rotation of the rotational head was conducted by defining the angular velocity $\omega = 628.31$ rad/s, with a vector lying on the axis X. In addition, density of the rotational head was increased in order to reflect the moment of inertia acting on the shaft of the device. Constrains applied to the pushing part only permit movement along the axis of the model and constraining movements in directions Y and Z (W2). Pressure realized by the hydraulic cylinder was imposed via force with a value estimated in experimental studies, i.e. 850 N. The FE model, together with the adopted boundary conditions is shown in Fig. 11.

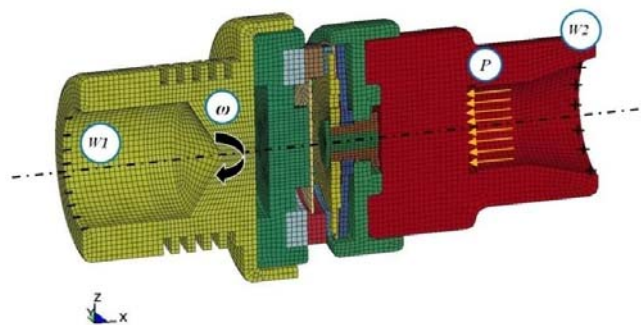


Fig. 11. Boundary conditions applied to the FE model of stand.

During braking, the kinetic energy is converted into heat in the mechanical construction of the brake. Part of this heat is transferred out of the system due to convection and radiation. All three components are included in the following relation:

$$F_f \frac{dS}{dt} = mc_p \frac{dT}{dt} + hA(T - T_0) + A\sigma T^4 \quad (1)$$

In the equation above: F_f - friction force, S - distance, m - mass, c_p - specific heat, T - temperature, h - heat transfer coefficient, T_o - ambient temperature, t - time, σ - Stefan-Boltzman const.

Analyses were conducted with assumption that both convection (second term) and radiation (third term) can be neglected, since only first stage of braking process was covered by the analyses. In other words, the only source of heat in the model was friction and whole work done by friction forces was converted into the thermal energy as equation:

$$F_f \frac{dS}{dt} = mc_p \frac{dT}{dt} \tag{2}$$

Friction force F_f was derived from well-known Coulomb model of friction with smoothing parameter stabilizing transition between static and dynamic friction. Contact normal force – a prerequisite for the friction force calculation – was obtained using the penalty function contact algorithm [22]. After several tests, explicit integration scheme was chosen to solve system of equations. One the main reason of that choice was the fact, that implicit methods were not noticeably faster.

5. Analysis of numerical simulations results

With a stable integration time step at the level of $5.5 \cdot 10^{-8}$ s, it took about week to cover first stage of braking process. In fact, total CPU time to cover 2 s of analysis period, was estimated at the level of 62 500 hours. It should be noted, that due to nature of the simulated problem, simplification of FE model was impossible. Fig.12 shows temperature distribution in the lining after 0.1s. It can be seen that “attacking” sides of pads are generating more heat than “trailing” sides, which is consistent with the observed behavior on the test stand.

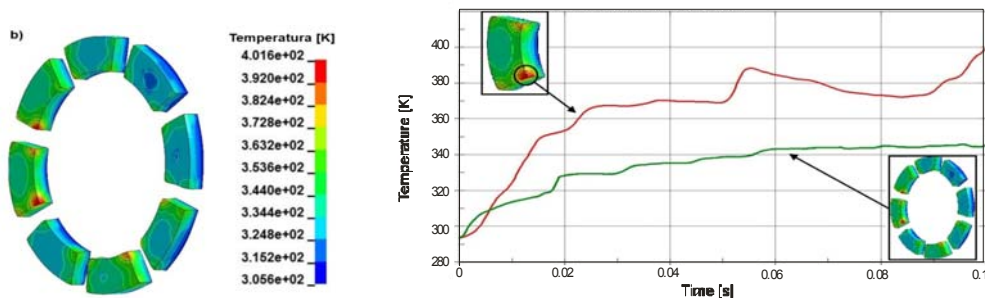


Fig.12. Temperature distribution on pads, at time $t = 0.1$ s

Fig. 13 shows temperature and friction force change over the time, where temperature was converted from °K to °C. Looking at the peak force values and temperature change for the same time moment, one can observe correlation between both quantities, as it was described by equation 2.

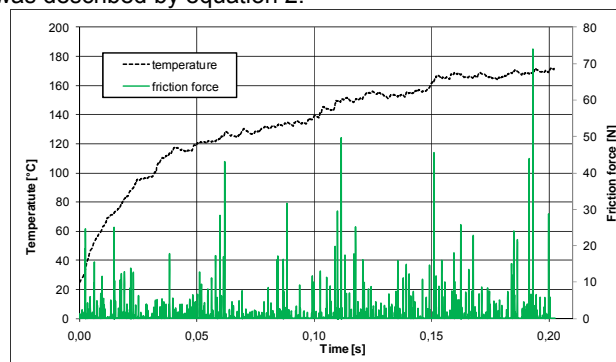


Fig. 13. Temperature and friction force versus time

The nature of changes in friction force values points to yet another difficulty associated with numerical analysis of the braking process - the level of discretization of contact surfaces. Very uneven and rapid change of the contact force shows that the finite element mesh could have been too coarse. On the other hand, further decreasing of the element size would have resulted in further decreasing of time step making FE calculations unfeasible. One of the ideas of avoiding this problem is to use meshless methods, e.g. SPH approach. Another advantage of SPH usage is possibility to include in the model micro structural phenomena, such as wear due to local surface imperfection [22].

It should be noted that, despite all the difficulties mentioned above and lack of the overlap time range between FE results and measurements, temperature calculated using FE method approaches the values measured experimentally, achieving 170°C at 0.2s (compared to 250°C at 0.3s). This indicates, that algorithm of thermomechanical

coupling, as well as the assumed method of conversion of mechanical energy into the thermal energy, are working correctly.

6. Conclusions

Numerical simulation of laboratory tests proved, that the application of FEM-based method is quite effective in simulating the transfer of kinetic energy into heat, which is the main energy transfer process during braking. In spite of aforementioned obstacles (mainly time-consuming calculations and discretization requirements for the contact surfaces) which temporarily prevented the calculations to cover the whole braking cycle thus making it impossible to directly compare the calculated and measured temperature data, it can be seen that the calculated temperature values (after the elongation of calculation period) will reach the level of measured ones. Currently conducted works are aimed at elongation of simulated brake process and implementation of SPH method for the modeling of brake pads operation. Additionally, on the basis of initial analyses, prediction of temperature values likely to occur in the braking system and the technical specifications of available thermal cameras it was concluded that the camera with longwave IR MCT detector type should be used for future experiments. Such cameras have broader measurement range, but lower thermal resolution than currently used camera with InSb detector. However, during measurements with high dynamic range of temperature changes the resolution of MCT-type camera is quite sufficient. Broadening of the measurement range will make it possible to compare the simulation and experimental results from the very beginning of brake process. Despite some problems with the saturation of camera detectors the thermal imaging proved its usefulness as a measurement technique for the recording of temperature values during brake examination. The measurement of a strictly defined part of a brake disc require some modification of test stand and the application of a different, faster thermal camera with fast data link to the computer. Camera data acquisition should be synchronized with the braking process on the test stand. Tested surfaces should be (if possible) prepared for the measurements performed by a thermal camera. It includes the surface treating in order to obtain uniform structure or the application of special coatings, provided that it will not influence the brake operation, particularly the heat transfer.

Acknowledgment

The result presented in paper are supported by realization of the Project is co-financed by the European Regional Development Fund within the framework of the 2. priority axis of the Innovative Economy Operational Programme, 2007-2013, submeasure 2.1. "The development of centres with high research potential". Contract no. POIG.02.01.00-14-095/09.

REFERENCES

- [1] Dufrénoy, P., Bodovillé, G., Degallaix, G., "Damage mechanisms and thermomechanical loading of brake discs", *Eur. Struct. Integrity Soc.* 29, 167–176 (2002).
- [2] Anderson, A.E., Knapp, R.A., "Hot spotting in automotive friction systems", *Wear* 135 (1990) 319–337.
- [3] Eleod, A., Baillet, L., Berthier, Y., Torkoly, T., "Deformability of the near surface layer of the first body", *Elsevier Sci. Tribol.* 41, 123–132 (2003).
- [4] Dufrénoy, P., Weichert, D., "A thermomechanical model for the analysis disc brakes fracture", *J. Thermal Stress.* 26 (8), 815–828 (2003).
- [5] Eleod, A., Oucherif, F., Devecz, J., Berthier, Y., "Conception of numerical and experimental tools for study of the tribological transformation of surface TTS", *Elsevier Sci. Tribol.* 36, 673–782 (1998).
- [6] Kao, T., Richmond, J.W., Douarre, A., "Brake disc hot spotting and thermal judder: an experimental and finite elements study", *Int. J. Vehicle Des.* 23, 276–296 (2000).
- [7] Dufrénoy, P., Panier, S., Weichert, D., "On the hot spots on railway disc brakes", *Proc. of the European Braking Conference GRRT*, (1998).
- [8] Panier, S., Dufrénoy, P., Weichert, D., "An experimental investigation of hot spots in railway disc brakes", *Wear* 256, 764–773 (2004).
- [9] Siroux, M., Harmand, S., Desmet, B., "Experimental study using infrared thermography on the convective heat transfer of a TGV brake disc in the actual environment", *Optical Eng.* 41 (7), 1558–1564 (2002).
- [10] Bauer, W., Oertel, H., Rink, M., "Spectral emissivity of bright and oxyded metals at high temperatures", *Fifteen Symposium on Thermophysical Properties*, Boulder, (2003).
- [11] Thevenet, J., Siroux, M., Desmet, B., "Measurements of brake disc surface temperature and emissivity by two-colour pyrometry", *Appl. Thermal Eng.* 30, 753–759 (2010).
- [12] Kasem, H., Thevenet, J., Boidin, X., Siroux, M., Dufrénoy, P., Desmet, B., Desplanques, Y., "An emissivity-corrected method for the accurate radiometric measurement of transient surface temperatures during braking", *Tribol. Inter.* 43, 1823–1830 (2010).
- [13] Madura, H., Kastek, M., Piątkowski, T., "Automatic compensation of emissivity in three-wavelength pyrometers", *Infrared Physics & Technology* vol. 51, 1-8 (2007).
- [14] Madura, H., Kastek, M., Sosnowski, T., Orzanowski, T., "Pyrometric method of temperature measurement with compensation for solar radiation", *Metrology and Measurement Systems* Vol. XVII no. 1, 77-86 (2010).

- [15] Uetz, H., Föhl, J., "Wear as an energy transformation process", *WEAR*, 253-264 (1978).
- [16] Kenedy, F. E., "Thermal and thermomechanical effects in dry sliding", *WEAR*, 100, 453-476, (1984).
- [17] Suii, N.P., Sin, H.C., "The genesis of friction", *WEAR* 69, 91-114 (1981)
- [18] Baranowski, P., Damziak, K., Malachowski, J., Mazurkiewicz, L., Kastek, M., Piatkowski, T., Polakowski, H., "Experimental and numerical tests of thermo-mechanical processes occurring on brake pad lining surfaces", *Surface Effects and Contact Mechanics X Vol. 71*, 15-24, (2011).
- [19] Piatkowski, T., Polakowski, H., Hots, N., "Examination of metallic surfaces for IR gray body sources", *Proc. of the Int. 9th Conf. Quantitative Infrared Thermography QIRT2008*, 185-190 (2008).
- [20] Bielecki, Z., Chrzanowski, K., Matyszek, R., Piatkowski, T., Szulim, M., "Infrared pyrometer for temperature measurement of objects of both wavelength- and time-dependent emissivity", *Optica Applicata Vol. 29* (3), 284-292 (1999).
- [21] Hallquist, J., "LS-DYNA Theory Manual", LST Co., (2005).
- [22] Baranowski, P., Damaziak, K., Malachowski, J., "Analysis of a brake including thermomechanical coupling" *Proc. of the 19th Int. Conf. On Computer Methods in Mechanics*, 123-124 (2011).